molecular pharmaceutics

articles

Paclitaxel Nanocrystals for Overcoming Multidrug Resistance in Cancer

Yang Liu, Leaf Huang, and Feng Liu*

Division of Molecular Pharmaceutics, Eshelman School of Pharmacy, University of North Carolina at Chapel Hill, Chapel Hill, North Carolina 27599-7360

Received January 19, 2010; Revised Manuscript Received April 14, 2010; Accepted April 26, 2010

Abstract: Here we described a paclitaxel (PTX) nanocrystal formulation using D-α-tocopheryl polyethylene glycol 1000 succinate (TPGS) as the sole excipient for overcoming multidrug resistance (MDR), a key challenge in current cancer therapy. To the best of our knowledge, it is the first report on PTX nanocrystals which can reverse MDR. TPGS serves as a surfactant to stabilize the nanocrystals and a P-gp inhibitor to reverse MDR. The size and morphology of the nanocrystals were studied by transmission electron microscopy, and the crystalline structure was determined by powder X-ray diffraction. An in vitro drug release profile showed that the nanocrystals exhibited sustained release kinetics compared to Taxol, which is the clinical paclitaxel formulation. The cytotoxicity and antitumor efficacy in xenograft models were also investigated. It is demonstrated that PTX/TPGS nanocrystals have significant advantages over Taxol in achieving better therapeutic effect in Taxol-resistant cancer cells both in vitro and in vivo, which was also confirmed by apoptosis assays. We envision that further development of this type of nanocrystal will provide a novel strategy for drug delivery and multidrug resistance treatment.

Keywords: Multidrug resistance; paclitaxel; nanocrystals; TPGS; cancer

Introduction

Paclitaxel (PTX) is a potent antineoplastic agent against a wide variety of malignancies.[1] It has been approved by the US FDA for the treatment of breast cancer, ovarian cancer and non-small-cell lung cancer (NSCLC).[2] However, multidrug resistance (MDR) developed by cancer cells still represents a major challenge in the clinical cure of cancer by PTX alone or in combination with other antineoplastic agents, especially advanced and metastatic forms. Elevated expression and activity of the ATP-binding cassette (ABC) transporter has been identified as an important reason for the failure of PTX-based treatments.[3] In the ABC superfamily, P-gp plays a key role in mediating the highest resistance to bulky anticancer agents.[4] It is a well-characterized transportor which is widely overexpressed in both solid tumors and hematological malignancies with a broad spectrum of substrate specificity.[5] Functioning as a drug efflux pump, P-gp prevents cytotoxic agents from reaching effective concentrations within cells. PTX has been shown to be a high affinity substrate a P-glycoprotein encoded by the multidrug resistance 1 (MDR1) gene, which hinders its successful therapy in cancers. To address this problem, P-gp inhibitors such as verapamil, quinine and cyclosporin A have been introduced to reverse MDR since the early 1980s.[6] However, clinical trials failed to show significant benefit.

* Corresponding author. Division of Molecular Pharmaceutics, University of North Carolina, Eshelman School of Pharmacy, Chapel Hill, NC 27599. Tel: (919)843-2277. Fax: (919)966-0197. E-mail: fliu@email.unc.edu.

(1) Schiff, P. B.; Fant, J.; Horwitz, S. B. Promotion of microtubule assembly in vitro by taxol. *Nature* **1979**, *277*, 665–667.

(2) Stinchcombe, T. E. Nanoparticle albumin-bound paclitaxel: a novel Cremphor-EL-free formulation of paclitaxel. *Nanomedicine (London, U.K.)* **2007**, *2*, 415–423.

(3) Bates, S. E.; Robey, R.; Miyake, K.; Rao, K.; Ross, D. D.; Litman, T. The role of half-transporters in multidrug resistance. *J. Bioenerg. Biomembr.* **2001**, *33*, 503–511.

(4) Borst, P.; Elferink, R. O. Mammalian ABC transporters in health and disease. *Annu. Rev. Biochem.* **2002**, *71*, 537–592.

(5) Szakacs, G.; Jakab, K.; Antal, F.; Sarkadi, B. Diagnostics of multidrug resistance in cancer. *Pathol. Oncol. Res.* **1998**, *4*, 251–257.

10.1021/mp100012s
Published on Web 04/26/2010

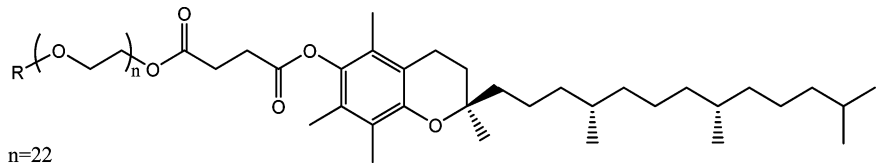

Figure 1. Structure of D-α-tocopheryl polyethylene glycol 1000 succinate (TPGS).

The efficacy of these inhibitors was largely compromised by pharmacokinetics interactions and increased side effects.[7,8]

Another limitation of the clinical application of PTX is its low solubility in water (<1 μg/mL). Currently, two commercially available formulations of PTX are Taxol and Abraxane. Taxol is based on a 1:1 (v/v) mixture of polyoxyethylated castor oil (Cremophor EL or simply Cremophor) and dehydrated ethanol. Notably, Cremophor is responsible for some severe side effects such as hypersensitivity reaction and peripheral neurotoxicity.[9] To address these issues, Abraxane was approved by the US FDA in 2005. This Cremophor-free formulation delivers PTX as a suspension of albumin particles in saline, which eliminates the solvent-related toxicities.[10] However, the preparation of Abraxane requires high-pressure homogenization of PTX in the presence of human serum albumin, resulting in the high cost of the dosage form.[11] Most importantly, there is no evidence that Abraxane has activities against MDR tumors. Thus, novel Cremophor-free formulations of PTX for overcoming MDR are still highly desirable.

Nanotechnology offers an unprecedented opportunity in drug delivery to tumors. These nanobased delivery systems provide many promising features for overcoming MDR: enhanced delivery to tumor tissues, optimized pharmacokinetics and delivery of multiple therapeutic agents in a single formulation.[12] In this study paclitaxel (PTX) nanocrystals were prepared using D-α-tocopheryl polyethylene glycol 1000 succinate (TPGS) as the sole excipient (Figure 1). TPGS was selected for this study for several reasons. First, it has been recognized as one of the most potent P-gp inhibitors among many different surfactants, which can function at a concentration well below critical micelle concentration (CMC).[13,14] Second, it has long-standing safety record in biomedical applications as a water-soluble derivative of natural vitamin E. In addition, TPGS lacks unrelated pharmacological effects and shows no pharmacokinetic interactions with other drugs.

Experimental Section

Material and Experimental Animals. Paclitaxel (PTX) was bought from Lc Laboratories (Woburn, MA). TPGS was bought from Eastman (Anglesey, U.K.). Pluronic F-127 (F127) and Cremophor-EL were purchased from Sigma-Aldrich (St. Louis, MO).

Female BALB/c nude mice (5 weeks old) were purchased from National Cancer Institute, U.S. National Institutes of Health (NCI, Frederick, MD). All work performed on animals was in accordance with and permitted by the University of North Carolina Institutional Animal Care and Use committee.

Resistant human ovarian cancer cell line, NCI/ADR-RES, was a kind gift from Dr. Russell Mumper (UNC—Chapel Hill, Chapel Hill, NC). Cells were maintained in Dulbecco's modified Eagle medium (DMEM) GlutaMAX medium (Invitrogen, Carlsbad, CA) supplemented with 10% fetal bovine serum (Invitrogen, Carlsbad, CA), 100 U/mL penicillin, and 100 μg/mL streptomycin (Invitrogen, Carlsbad, CA). Human lung cancer cell line, NCI-H460, and human nasopharynx carcinoma cell line, KB, cells were obtained from American Type Culture Collection. Cells were maintained in RPMI-1640 medium supplemented with 10% fetal bovine serum (Invitrogen, Carlsbad, CA), 100 U/mL penicillin, and 100 μg/mL streptomycin (Invitrogen, Carlsbad, CA).

Preparation of Nanocrystals. The nanocrystals were prepared by the method of the stabilization of nanocrystal (SNC).[15] Briefly, PTX and TPGS were first dissolved in

(6) Nobili, S.; Landini, I; Giglioni, B.; Mini, E. Pharmacological strategies for overcoming multidrug resistance. *Curr. Drug Targets* **2006**, *7*, 861–879.
(7) Baer, M. R.; George, S. L.; Dodge, R. K.; O'Loughlin, K. L.; Minderman, H.; Caligiuri, M. A.; Anastasi, J.; Powell, B. L.; Kolitz, J. E.; Schiffer, C. A.; Bloomfield, C. D.; Larson, R. A. Phase 3 study of the multidrug resistance modulator PSC-833 in previously untreated patients 60 years of age and older with acute myeloid leukemia: Cancer and Leukemia GroupB Study 9720. *Blood* **2002**, *100*, 1224–1232.
(8) Szakacs, G.; Paterson, J. K.; Ludwig, J. A.; Booth-Genthe, C.; Gottesman, M. M. Targeting multidrug resistance in cancer. *Nat. Rev. Drug Discovery* **2006**, *5*, 219–234.
(9) Gelderblom, H.; Verweij, J.; Nooter, K.; Sparreboom, A. Cremophor EL: the drawbacks and advantages of vehicle selection for drug formulation. *Eur. J. Cancer* **2001**, *37*, 1590–1598.
(10) Nyman, D. W.; Campbell, K. J.; Hersh, E.; Long, K.; Richardson, K.; Trieu, V.; Desai, N.; Hawkins, M. J.; Von Hoff, D. D. Phase I and pharmacokinetics trial of ABI-007, a novel nanoparticle formulation of paclitaxel in patients with advanced nonhematologic malignancies. *J. Clin. Oncol.* **2005**, *23*, 7785–7793.
(11) Hennenfent, K. L.; Govindan, R. Novel formulations of taxanes: a review. Old wine in a new bottle? *Ann. Oncol.* **2006**, *17*, 735–749.
(12) Jabr-Milane, L. S.; van Vlerken, L.E.; Yadav, S.; Amiji, M. M. Multi-functional nanocarriers to overcome tumor drug resistance. *Cancer Treat. Rev.* **2008**, *34*, 592–602.
(13) Dintaman, J. M.; Silverman, J. A. Inhibition of P-glycoprotein by D-alpha-tocopheryl polyethylene glycol 1000 succinate (TPGS). *Pharm. Res.* **1999**, *16*, 1550–1556.
(14) Xu, P.; Gullotti, E.; Tong, L.; Highley, C. B.; Errabelli, D. R.; Hasan, T.; Cheng, J. X.; Kohane, D. S.; Yeo, Y. Intracellular drug delivery by poly(lactic-co-glycolic acid) nanoparticles, revisited. *Mol. Pharmaceutics* **2009**, *6*, 190–201.
(15) Liu, F.; Park, J. Y.; Zhang, Y.; Conwell, C.; Bathula, S. R.; Huang, L. Targeted cancer therapy with novel high drug-loading nanocrystals. *J. Pharm. Sci.* **2010**, DOI 10.1002/jps.22112.

chloroform (in a glass tube) with different ratios (1:1−1:5, w/w) and coprecipitated by evaporating the chloroform with a steady flow of nitrogen gas. A trace amount of chloroform was removed by keeping the precipitates under a vacuum in a desiccator for 2 to 4 h. Following 20 min hydration in water and vortex, suspensions were sonicated for 10 to 15 min in a bath-type sonicator (output 80 kC, 80 W) to form nanocrystals.

Characterization of Nanocrystals. Particle size and morphology were determined by transmission electron microscope (TEM) with an acceleration voltage of 100 kV. To prepare the samples, PTX/TPGS nanoparticle nanocrystals (5 μL) were deposited onto a 200 mesh copper grid coated with carbon (Ted Pella, Inc., Redding, CA) and allowed to stand for 5 min, and excess liquid was wicked off. Samples were stained with 1% uranyl acetate (5 μL), followed by overnight air drying at room temperature. Images were acquired using a JEOL 100CX II TEM.

The structure of PTX/TPGS nanocrystals was studied by powder X-ray diffraction (XRD). PTX/TPGS nanocrystal suspension was lyophilized to obtain powder. Pure PTX crystals were prepared using the same method. Then the XRD diagrams were collected in a Rigaku Multiflex powder diffractometer.

To assess the release kinetics, dialysis cassettes (molecular weight cutoff 10,000 Da) were filled with 1 mL of different PTX formulations and immersed in 400 mL of dialysis buffer (PBS (pH 7.4) containing 0.05% Tween 80). Taxol which is the clinical paclitaxel formulation in Cremophor EL and dehydrated USP-grade ethanol (1:1, v/v) was used as a control. At designated time points, aliquots of 2 mL of buffer were sampled and replaced with the same volume of fresh dialysis buffer. The whole volume of dialysis buffer was replaced at selected time intervals to maintain a sink condition. One microgram (10 μL) of *n*-butyl *p*-hydroxybenzoate was added to the aliquots as an internal standard (STD). PTX and STD were extracted by a liquid−liquid extraction with methyl *tert*-butyl ether. After the evaporation of methyl *tert*-butyl ether by nitrogen stream, the residue was dissolved with the mobile phase (methanol:water = 80:20) and quantified by HPLC. The HPLC system was performed at a flow rate of 1.0 mL/min at 228 nm with a UV detector, using a 25 mm × 4.6 mm reverse phase C18 column.

The stability of PTX/TPGS nanocrystals was investigated at room temperature and 37 °C. PTX/F127 nanocrystals which were developed in our lab previously served as a control. At intervals of specified time, the particle size and distribution of nanocrystals were measured using a submicron particle sizer (NICOMP particle sizing systems, Autodilute-PAT model 370, Santa Barbra, CA) in the NICOMP mode.

Cytotoxicity on Sensitive and Resistant Cancer Cells. To evaluate cytotoxicity of PTX/TPGS nanocrystals, MTT (3-[4,5-dimethylthiazole-2-yl]-2,5-diphenyl-tetrazolium bromide) assay was performed on NCI/ADR-RES, KB and H460 cells. Briefly, cells were seeded into 96-well plates at a concentration of 1×10^4 cells/well in a volume of 200 μL/well. After 24 h, the medium was removed and 200 μL of fresh medium containing 5 μM PTX in various formulations was added, including PTX/TPGS nanocrystals, PTX/F127 nanocrystals, Taxol and free PTX. Free PTX was prepared by dissolving PTX in chloroform and processing by the method of SNC as described above except without TPGS. To study the influence of the amount of surfactant on cytotoxicity, fresh medium containing PTX/TPGS nanocrystals and PTX/TPGS mixture with different drug/surfactant ratios was added, where PTX concentration was kept at 10 μM. Dose dependent cytotoxicity of various PTX formulations was also evaluated, including PTX/TPGS nanocrystals, PTX/F127 nanocrystals, Taxol and free PTX. Following a 43 h period of incubation, 5 μL of MTT (5 mg/mL) was added to each well. The plates were incubated for an additional 5 h. Then the supernatants were carefully aspirated, and 200 μL of dimethyl sulfoxide was added to each well to dissolve the crystal product. The absorbance values were read on a microplate reader using a Bio-Rad microplate imaging system (Hercules, CA) at a wavelength of 570 nm. Cell viability was calculated using the following formula: viability % = (A570 nm for the treated cells/A570 nm for the control cells) × 100, where A570 nm is the absorbance.

Assessment of Apoptosis by Annexin-V/PI Staining. Cellular apoptosis was assessed using flow cytometry. In brief, NCI/ADR-RES cells were seeded in a 6-well plate at a concentration of 2×10^5 cells/well. 24 h later, PTX/TPGS nanocrystals, Taxol, TPGS and PBS were added. PTX concentration was 5 μM in both PTX/TPGS nanocrystals and Taxol. In the surfactant alone group, TPGS concentration was the same as that in the PTX/TPGS nanocrystal group. After 48 h treatment, the cells were harvested, washed and stained with annexin-V/propidium iodide (PI) according to the manufacturer's instruction. Apoptotic cells were measured by BD FACS Canto flow cytometer (BD Biosciences, San Jose, CA).

In Vivo Anticancer Effects. 5×10^6 NCI/ADR-RES cells were injected subcutaneously into the right flanks of nude mice for inoculation. Once the tumor mass in the xenograft was established, mice were randomly assigned to treatment groups (5 mice per group) and intravenously injected with different formulations of PTX at a dose of 10 mg/kg each single dose or TPGS alone at a dose of 50 mg/kg each single dose. 50 mg/kg of TPGS was given in order to keep consistent with the drug/surfactant ratio used in in vitro studies. Treatments were conducted on day 0, 3, 6, 9, 12. Tumor volume was measured every other day, calculated as (length × width^2)/2. Mice were sacrificed when the long dimension of the tumor reached 2 cm.

Statistics. Data are presented as the mean ± standard deviation. One-way analysis of variance (ANOVA) was used to determine significance among groups in animal studies. For stability and cytotoxicity studies, statistical analyses were performed by a two-tailed Student *t* test. A value of $p < 0.05$ was considered to be significant.

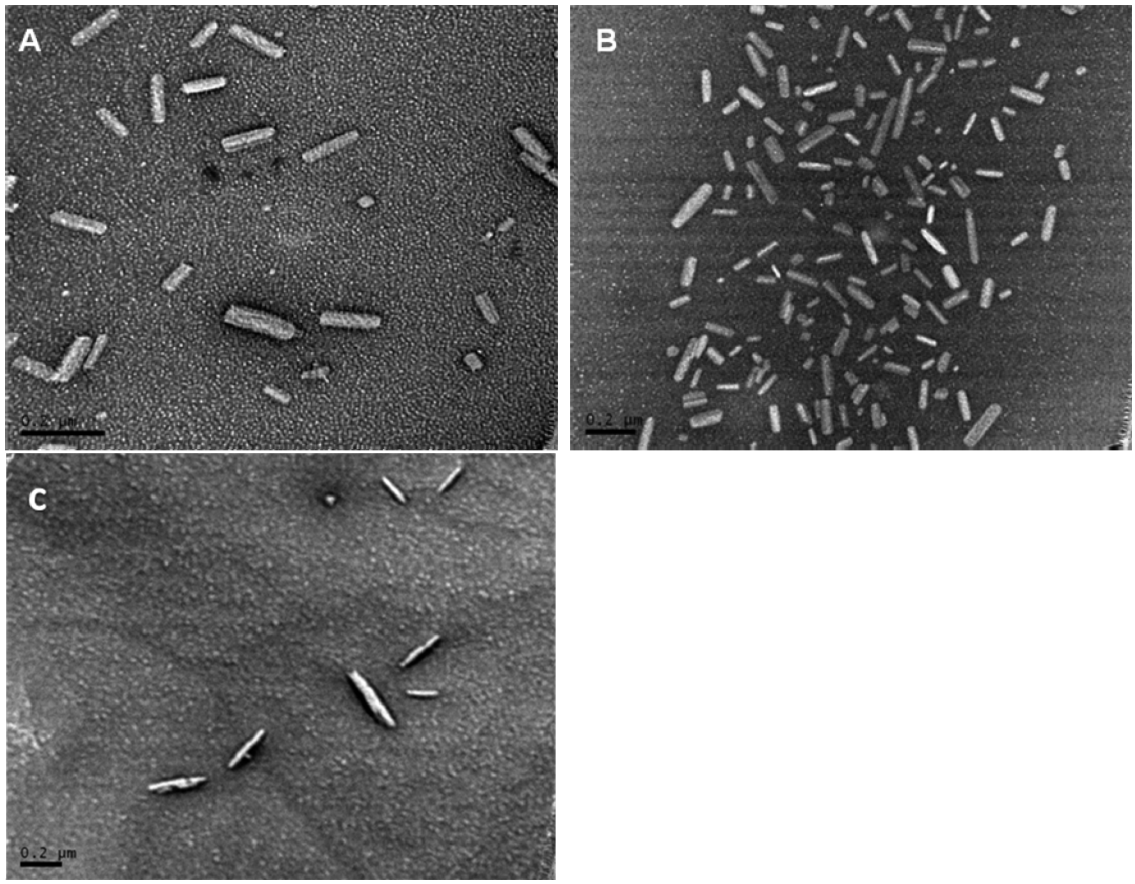

Figure 2. Transmission electron microscope images of PTX formulations. A: PTX/TPGS nanocrystals with the ratio of 1:1 (w/w). B: PTX/TPGS nanocrystals with the ratio of 1:5 (w/w). C: Itraconazole/TPGS particles with the ratio of 1:5 (w/w). Scale bars represent 200 nm.

Results

Characterization of PTX/TPGS Nanocrystals. PTX/TPGS nanocrystals were prepared using TPGS as the single excipient. Different drug/surfactant ratios were investigated (1:1−1:5, w/w). The results showed that the ratio did not affect the size and morphology of the nanocrystals. Figures 2A and 2B show PTX/TPGS nanocrystals with boundary drug/surfactant ratios (1:1 and 1:5, w/w). They all exhibited a rod shape with moderate uniform particle size. The average width is about 40 nm, and the length is around 150 nm. When the ratio was lower than 1/1 (further decrease of the amount of TPGS), the nanocrystals could not be formed. Thus, the maximum drug loading ratio of the TPGS nanocrystals was found to be as high as 50%. TPGS can also form nanoparticles with other hydrophobic drugs such as itraconazole, as shown in Figure 2C, indicating a broader application.

XRD was performed to study the structure of the rod-shaped particles. As shown in Figure 3, the presence of a large number of Bragg peaks in the diffraction patterns is indicative of a crystalline structure. Although pure PTX has a fairly flat background and sharper peaks than PTX/TPGS nanocrystals, the two diagrams are very similar and almost superimposable.

The in vitro drug release profile of PTX/TPGS nanocrystals was assessed in an effort to determine whether PTX would be released from nanocrystals prior to cellular uptake. As depicted in Figure 4, PTX/TPGS nanocrystals have a substantially sustained release profile compared with Taxol. The cumulative release of PTX after 72 h was about 50% from PTX/TPGS nanocrystals. While in Taxol, PTX was encapsulated in micelles of Cremophor, resulting in a rapid release (100% within 22 h). No initial burst release of PTX was observed for nanocrystals, which indicated that PTX was not likely to be present at or near the surface of the nanocrystals. Instead PTX was shelled by the nonionic surfactants coated on the surface of the nanocrystals. This assumption was supported by X-ray photospectrometer (XPS). To prove the successful surface coating of TPGS on PTX, the nitrogen atom which only exists in PTX molecules was specifically scanned and the absence of a nitrogen signal verified the coating. Pure PTX crystals exhibited a relatively rapid release, which is understandable, because there is not any surfactant coated on the surface.

The particle size of nanocrystals was measured to evaluate the stability. As shown in Figure 5, the size of PTX/TPGS nanocrystals remained stable at room temperature for more than two weeks, while the size of PTX/F127 nanocrystals dramatically increased. Moreover, PTX/TPGS nanocrystals are stable

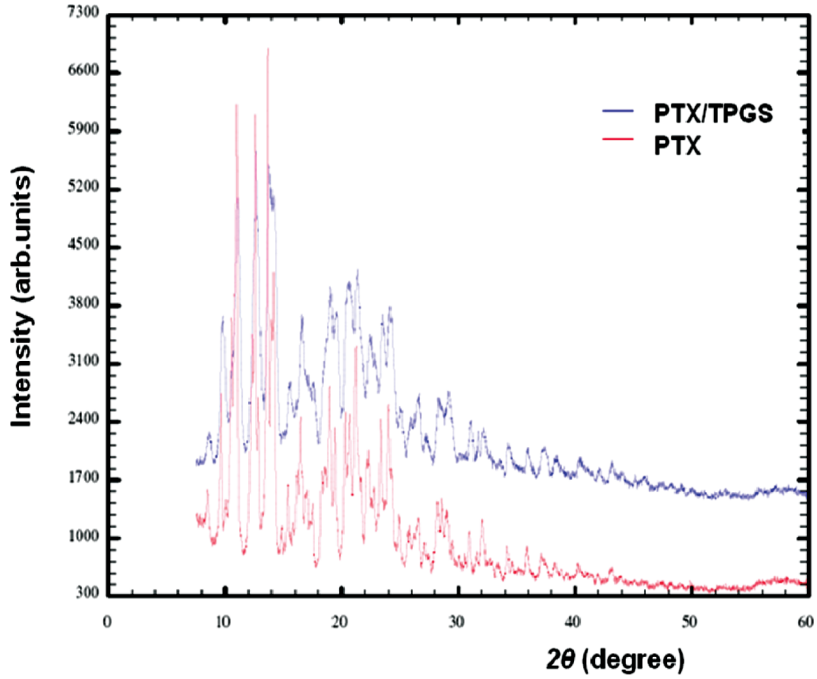

Figure 3. Powder XRD patterns of pure PTX crystals and PTX/TPGS nanocrystals.

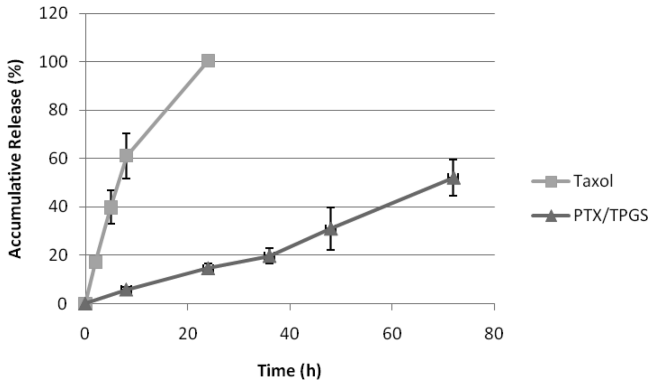

Figure 4. In vitro release profiles of PTX from Taxol and PTX/TPGS nanocrystals.

at 37 °C for 5 days while PTX/F127 nanocrystals aggregated within hours. The drug/surfactant ratio did not affect the thermostability since 1:1 and 1:5 (w/w) PTX/TPGS nanocrystals exhibited comparable stability, as shown in Figure 4B.

Effect on Sensitive and Resistant Cancer Cells in Vitro. Figure 6 summarizes the antiproliferation effect of various formulations of PTX on a panel of human cancer cells. In KB and H460 cells, PTX/TPGS nanocrystals, PTX/F127 nanocrystals, Taxol and free PTX all greatly inhibited cell proliferation. There was not any significantly difference among the four treatments. However, in NCI/ADR-RES cells, which overexpress P-gp and are resistance to PTX, PTX/F127 nanocrystals and free PTX become almost ineffective. Taxol had a moderate inhibition of cell growth in resistant cells. PTX/TPGS nanocrystals exhibited a significantly enhanced antiproliferation effect in NCI/ADR-RES cells over other formulations, which inhibited cell growth by 40%, as shown in Figure 6A. The amount of surfactant affected cytotoxicity of PTX/TPGS nanocrystals in NCI/

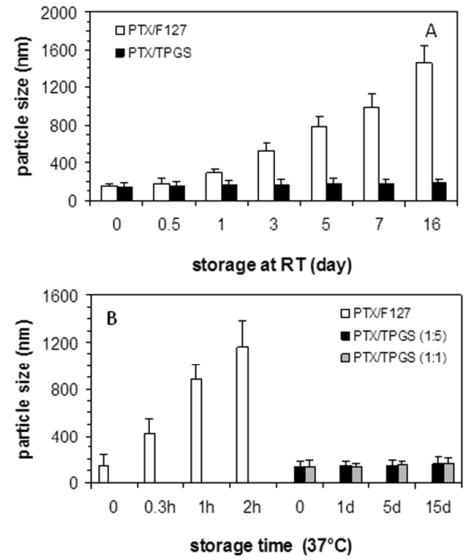

Figure 5. Stability of PTX/TPGS nanocrystals. (A) PTX/F127 nanocrystal size increased upon storage at room temperature while PTX/TPGS nanocrystal size remained the same. (B) PTX/F127 nanocrystal size increased at 37 °C while PTX/TPGS nanocrystal size remained the same. (PTX = 586 μM.)

ADR-RES cells. As shown in Figure 6B, as the amount of surfactant increased, the antiproliferation effect of PTX/TPGS nanocrystals increased, in either PTX/TPGS nanocrystals or mixture, indicating that TPGS is modulating drug resistance transporters. However, at low surfactant concentration, PTX/TPGS nanocrystals are more cytotoxic than PTX/TPGS mixture, whereas at high surfactant concentration they are comparable. In the dose dependent assay shown in Figure 6C, PTX/F127 nanocrystals or free PTX alone did not show significant inhibition in NCI/ADR-RES cells even at a

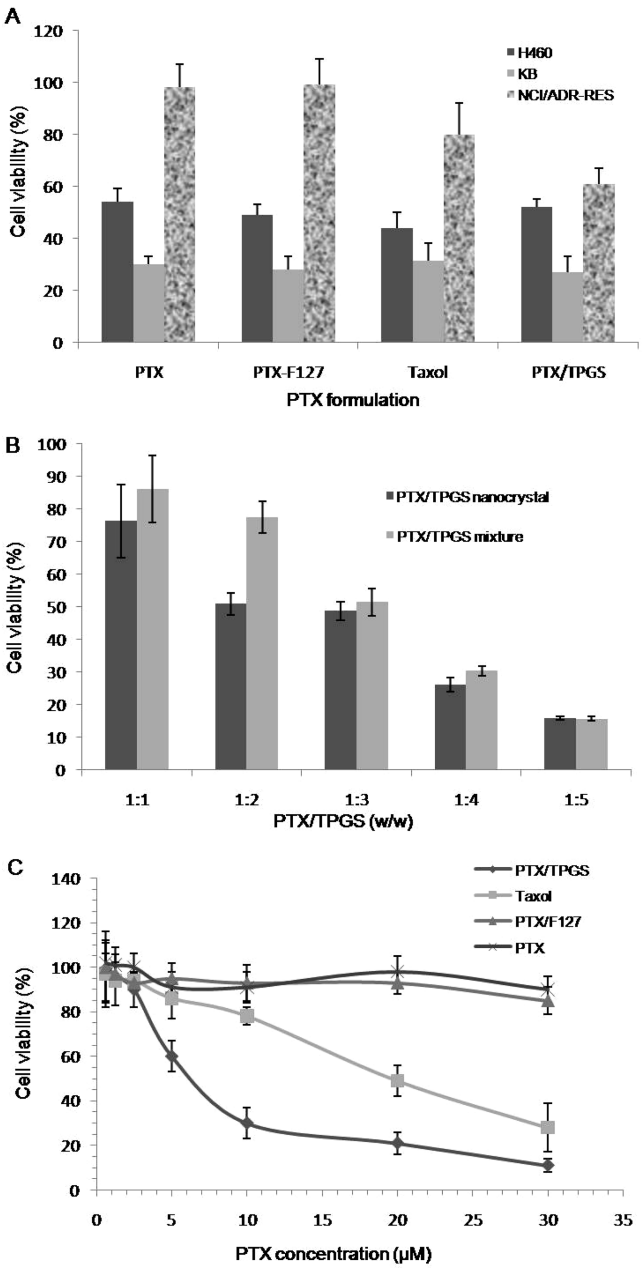

Figure 6. Cell viability after being treated with different formulations for 48 h. A: Effects of PTX/TPGS nanocrystals, PTX/F127 nanocrystals, Taxol and PTX at the same 5 μM PTX concentration on NCI/ADR-RES, KB and H460 cells. B: Effects of PTX/TPGS nanocrystals (10 μM) with different amount of TPGS and PTX/TPGS mixture (10 μM) with different amount of TPGS. C: Dose-dependent response of PTX/TPGS nanocrystals, PTX/F127 nanocrystals, Taxol and PTX on NCI/ADR-RES cells.

concentration of 30 μM. However, PTX/TPGS nanocrystals could effectively reverse the resistance and inhibited cell growth with an IC_{50} around 5 μM. Taxol can also overcome the resistance but is less effective than PTX/TPGS nanocrystals.

Apoptosis Assay in Resistance Cancer Cells. Since apoptosis is the predominant mechanism of cell death in response to taxane chemotherapy,[16] apoptosis-inducing effect of nanocrystals was assessed using Annexin-V/PI staining. Apoptotic percentages were calculated based on the cells stained with annexin-V (FITC) alone (early apoptosis) and doubly stained with both annexin V and PI (late apoptosis). It was shown that all the treatment could induce certain amounts of apoptosis in NCI/ADR-RES cells (Figure SI1 in the Supporting Information). For example, the early and late apoptosis percentages for Taxol were 19.4% and 7.1%, respectively. TPGS alone can also induce 11.4% of early apoptosis and 18.6% of late apoptosis. However, PTX/TPGS nanocrystals showed the most significant apoptosis-inducing effect. After applying PTX/TPGS nanocrystals, the apoptotic percentage dramatically increased to more than 95%. This result was consistent with the cytotoxicity results above.

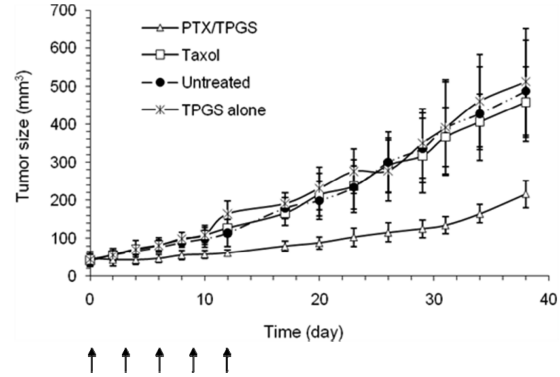

Figure 7. Tumor growth inhibition effect of PTX/TPGS nanocrystals, Taxol and TPGS alone in the NCI/ADR-RES xenograft model. Solid arrows indicate the days of intravenous administration.

Antitumor Efficacy in Tumor Xenograft Models. Figure 7 describes the therapeutic efficacy following applying various formulations to the NCI/ADR-RES xenografts in nude mice. TPGS alone did not show any significant antitumor efficacy in vivo. Even Taxol given at a dose of 10 mg/kg was generally ineffective in inhibiting tumor growth, indicating that NCI/ADR-RES xenografts are truly resistant. However, an obvious tumor regression was observed in animals treated with10 mg/kg of PTX/TPGS nanocrystals, indicating a significantly enhanced tumor inhibition effect over Taxol ($p < 0.01$), as shown in Figure 7.

Body weight of mice was also measured throughout the study. No weight loss occurred in the mice treated with PTX/TPGS nanocrystals (data not shown), indicating that this formulation of PTX was well tolerated.

Discussion

As shown in the results, the TPGS based PTX nanocrystals reported here have several unique features. First, the stable PTX nanocrystals were formulated with a P-gp inhibitor (i.e., TPGS) as a sole excipient. The ability of overcoming MDR phenotype both in vitro and in vivo makes this formulation

(16) Wang, L. G.; Liu, X. M.; Kreis, W.; Budman, D. R. The effect of antimicrotubule agents on signal transduction pathways of apoptosis: a review. *Cancer Chemother. Pharmacol.* **1999**, *44*, 355–361.

more significant. Second, TPGS served dual functions in this formulation: stabilizing the nanocrystals and inhibiting P-gp activity. Third, the nanocrystals exhibited a high capacity of drug-loading compared to Taxol and Abraxane, which may lead to decreased infusion time or change of administration routine. Another advantage of nanoparticles which exhibit a high ratio of drug to excipient is that, upon entering the target cells, the nanoparticles will unload an increased amount of the drug to the cells and therefore maximize therapeutic efficacy. Moreover, since the preparation is easy to scale up and the excipient is readily available, the formulation is cost-effective and has a potential for development. TPGS stabilized and solubilized PTX nanocrystals by coating the outside, which was confirmed by XPS (data not shown). This stabilized crystalline structure prevents the nanocrystals from aggregation through storage and gives slow release kinetics.

In cytotoxicity study, it is not surprising to find that Taxol had some activity against resistant cells, although it was not as effective as PTX/TPGS nanocrystals, because Cremophor can modulate MDR by inhibition of the efflux pumps.[17] However, it is worth noticing that the concentration of Cremophor in Taxol was 16-fold higher than the concentration of TPGS in nanocrystals. It is not feasible to achieve such a high concentration in vivo to bring any clinical benefit since Cremophor is well-known for its toxicity. Apoptosis assay was also conducted, showing that PTX/TPGS nanocrystals were more potent than Taxol in killing tumor cells through the apoptosis-inducing mechanism, which is accepted as the predominant mechanism of cell death in response to taxane chemotherapy.[16] It appeared that TPGS alone could be slightly cytotoxic for in vitro study while in vivo results demonstrate that TPGS has no antitumor effect. This could be understood since surfactants at a relatively high concentration in in vitro study resulted in lysis of cells. Slow release rate of PTX from PTX/TPGS nanocrystals does not contradict its enhanced cytotoxicity since TPGS inhibits drug resistance transporters in a dose-dependent manner. Besides, nanocrystals can be internalized by cells via endocytosis, resulting in a higher intracellular concentration of PTX. The clear mechanism needs to be further elucidated by cellular uptake study. It was shown that, at high surfactant concentration, PTX/TPGS mixtures showed comparable cytotoxicity as PTX/TPGS nanocrystals. One possible explanation is that, at high concentration above critical micelle concentration of TPGS, extra TPGS starts to coat PTX and form micro- or nanocrystals during sonication. Therefore, the resulted formulation behaves more like nanocrystals rather than simple mixture.

PTX/TPGS nanocrystals exhibited a significant improved antitumor effect compared to Taxol in the Taxol-resistant NCI/ADR-RES cells especially in vivo. It could be attributed to the inhibition of P-gp function by TPGS, as we hypothesized in formulation design. Meanwhile, the slow release of PTX from the stabilized nanocrystals may lead to a longer half-life of PTX, resulting in enhanced efficacy. The nano size of the particles may also contribute to the antitumor effect, since it has long been established that small size particles intend to penetrate into interstitium of tumor through leaky vasculature.[18] As PTX and TPGS were codelivered in the same carrier simultaneously, they are more likely to have synergism in antitumor effects. Pharmacokinetics and biodistribution studies are needed to further elucidate the mechanism.

Generally speaking, when tumors develop resistance to a certain drug (about 50% of total cancer cases),[19] physicians have to switch to another chemotherapeutic agent or radiation to circumvent this resistance. To make things worse, cancer cells often develop resistance to different drugs, which was described above as MDR. PTX/TPGS nanocrystals overcome MDR elicited by PTX alone, providing an alternative for the treatment of MDR. A similar strategy to overcome MDR has been reported recently by Dong et al. using paclitaxel-loaded lipid-based nanoparticles which also include TPGS as one of the excipients.[20] A lot of cancer drugs, such as etoposide and camptothecin, are substrates of P-gp due to their hydrophobicity. Therefore, this approach could potentially extend to this type of drugs, where the issue of solubility and MDR could be addressed at the same time.

In conclusion, we have demonstrated that PTX/TPGS nanocrystals can provide a variety of benefits including high drug loading capacity, high stability, sustained release, and most importantly, the ability to overcome MDR both in vitro and in vivo. This nanoscaled formulation may provide a novel strategy for overcoming multidrug resistance in cancer therapy.

Acknowledgment. This study was supported by the National Institutes of Health (Grant CA129825). We thank Drs. Wallace Ambrose, Carrie Donley and Peter White for their help with this work.

Supporting Information Available: Apoptotic percentages were calculated based on the cells stained with annexin-V (FITC) alone (early apoptosis, Q4) and doubly stained with both annexin V and PI (late apoptosis, Q2). This material is available free of charge via the Internet at http://pubs.acs.org.

MP100012S

(17) Woodcock, D. M.; Linsenmeyer, M. E.; Chojnowski, G; Kriegler, A. B.; Nink, V.; Webster, L. K.; Sawyer, W. H. Reversal of multidrug resistance by surfactants. *Br. J. Cancer* **1992**, *66*, 62–68.

(18) Matsumura, Y.; Maeda, H. A new concept for macromolecular therapeutics in cancer chemotherapy: mechanism of tumoritropic accumulation of proteins and the antitumor agent smancs. *Cancer Res.* **1986**, *46*, 6387–6392.

(19) Gorre, M. E.; Mohammed, M.; Ellwood, K.; Hsu, N.; Paquette, R.; Rao, P. N.; Sawyers, C. L. Clinical resistance to STI-571 cancer therapy caused by BCR-ABL gene mutation or amplification. *Science* **2001**, *293*, 876–880.

(20) Dong, X; Mattingly, C. A.; Tseng, M. T.; Cho, M. J.; Liu, Y; Adams, V. R.; Mumper, R. J. Doxorubicin and paclitaxel-loaded lipid-based nanoparticles overcome multidrug resistance by inhibiting P-glycoprotein and depleting ATP. *Cancer Res.* **2009**, *69*, 3918–3926.